

## EXPERIMENTS ON SIMULTANEOUS SEA SOUNDING USING SHIPBOARD AND AIRBORNE LIDARS

I.E. Penner and V.S. Shamanaev

*Institute of Atmospheric Optics,  
Siberian Branch of the Russian Academy of Sciences, Tomsk  
Received October 26, 1993*

*The experiments were performed on simultaneous sea sounding using shipboard and airborne lidars. Hydrologic monitoring revealed the presence of local inhomogeneity in salinity. Not far from this place the airborne lidar recorded the presence of pulses from under the water with variable state of polarization at depths of 10–15 m. For regions with homogeneous water both lidars gave the radiation attenuation coefficients and depolarization profiles close in values.*

Widespread use of lidars for studying the sea water areas poses the problem of comparing the results obtained using different instruments. However, it should be noted that the lidar data are indirect, and when the inverse problem of sounding is solved, they are affected by the experimental conditions, i.e., specifications of lidars as well as light scattering properties of water.<sup>1–5</sup>

A full-scale metrological comparison of different lidars is a complicated and costly experiment. Nevertheless, at present the conduction of the experiments which can even partially solve this problem must not be ruled out.

We undertook such an investigation in collaboration with the administration of Sevrybpromrazvedka using the lidars developed at the Institute of Atmospheric Optics. The MAKREL'–2 lidar placed onboard an IL–18DORR aircraft and equipped with a photomultiplier FÉU–84–3 was used in the experiments.<sup>6</sup> A 2-channel 6-bit analog-to-digital converter with 25 ns quantization time was used for recording of the polarization components of a backscatter signal. The nadir sensing geometry was employed.

The SVETOZAR–3 lidar<sup>6,7</sup> was placed onboard the *Atlantik–733* scientific-research vessel. One of the three receiving telescopes of the lidar was used in these measurements. The signals were detected with the photomultipliers 28ÉLU–P15 and recorded by a multichannel 7-bit ADC with a 10–ns quantization step. The lidar was positioned in a cabin, and the sea was sounded using a deflecting mirror located overboard the vessel. The mirror was oriented to the plane of laser radiation polarization in such a way that its reflection matrix did not distort the sounding and received radiation pulses.<sup>7</sup>

The radiation attenuation coefficient was reconstructed by the method of logarithmic derivative

$$\varepsilon = \frac{n}{2(z_2 - z_1)} \ln \frac{F(z_1) \left( H + \frac{z_1}{n} \right)^2}{F(z_2) \left( H + \frac{z_2}{n} \right)^2}, \quad (1)$$

where  $H$  is the height of lidar location above the water,  $F(z)$  is the power of lidar return arriving from the depth  $z$  below the sea surface, and  $n$  is the sea–water refractive index.

The solution in the form of Eq. (1) is sensitive to the contribution of multiple scattering. Moreover, the value calculated using Eq. (1) can be closer to either scattering or absorption coefficients.<sup>8</sup> Therefore to maintain the

analogous conditions of multiple scattering for both lidars, their viewing angles varied. The parameter  $\eta = H \varepsilon \theta$  (where  $\theta$  is the viewing angle), describing the contribution of multiple scattering to the lidar return, was maintained approximately equal for both lidars.

The visibility depth of a white disk  $z_d$  and water temperature and salinity were measured using the shipboard lidar. The water homogeneity was monitored with a sonar. The scattering coefficient  $\sigma$  was calculated from the regression<sup>9</sup>

$$\sigma = 7.6 z_d^{-1} - 0.04. \quad (2)$$

It is valid in the wavelength range 520–550 nm with correlation coefficient for  $\sigma$  and  $z_d^{-1}$  being equal to 0.933 and rms error of 0.11 m<sup>-1</sup>.

There is another relation for the attenuation coefficient

$$\varepsilon = 7.0 z_d^{-1}, \quad (3)$$

when the wavelength is about 520 nm (see Ref. 10).

Over the ~50×50 km<sup>2</sup> water area centered at 72°20' N and 22°00' E the vessel deployed five research stations. Station 3 turned out to be the most appropriate one. In this region the aircraft with the lidar conducted several runs 30 km long being at a distance of 0.1–10 km from the vessel.

Unfavourable meteorological conditions (sea roughness index up to 5 and low cloudiness) resulted in the spread of the measured values of  $z_d$  within the limits 25–30 m. It is well known<sup>12</sup> that the accuracy of measurements of  $z_d$  for a sea roughness index of 4 is ±2 m. In our case this corresponds to  $\delta z_d \approx 8\%$ . (For very transparent water the conditions of illumination and physiological peculiarities of an eye are of great importance.)

Hence, the recalculation based on Eqs. (3) and (2) yielded  $\sigma = (0.26–0.21) \text{ m}^{-1}$  or  $\varepsilon = (0.28–0.23) \text{ m}^{-1}$ . In this case the photon survival probability  $\Lambda = \sigma/\varepsilon = 0.93–0.91$  can be considered to be overestimated for sea water.

The inversion of the shipboard lidar data yielded  $\varepsilon = (0.14 \pm 0.02) \text{ m}^{-1}$ . The standard deviation of the measured values of  $\varepsilon$  exceeded the calculational errors. For airborne lidar  $\varepsilon = (0.15 \pm 0.08) \text{ m}^{-1}$ . Thus the mean values of these quantities coincide while the spread of the data of airborne measurements is much greater. This is due to a larger measurement error of the 6-bit airborne ADC as

compared to the 7-bit shipboard ADC as well as due to a high-power fluctuating component of the signal of Fresnel reflection from the sea surface.

It is interesting to note a large systematic bias (by a factor of 1.5–2) of the values of  $\epsilon$  derived from lidar data from this quantity estimated by a conventional method. This bias coincides in magnitude with the Swedish data published in Ref. 11 in which the value of the scattering coefficient measured by independent reference instruments exceeded the corresponding value derived from lidar data.

The hydrological conditions in the region under study were characterized by uniform mixing of water masses of the southern wing of the Gulf Stream. The surface temperature of water along the ship's route varied by tenth fractions of a degree, the submerged temperatures at the same horizon varied by several hundredth of a degree. Salinity variations were of the same order of magnitude. Curves 1 and 2 in Fig. 1 show the variations in temperature and salinity at station 2 as a function of depth.

The analogous profiles, which indicate almost no change in salinity and temperature with depth, were obtained at the other stations except station 3. Near this station the profiles plotted by curves 3 and 4 were observed. Such a jump in salinity is termed a halocline<sup>13</sup> and its absolute value is 0.13 of a thousandth part here. The acoustic sounding at this place showed that in the region of halocline there are no coarse solid formations of biological or mineral origin. The upper 5-m layer was stable, i.e., well mixed due to wind-driven sea waves. It is notable that when going from station 3 to station 4, the depth of the sea bottom decreased from 400 to 150 m. This provides an explanation for the local density discontinuity since the region of an abrupt change in the sea depth is normally accompanied by the presence of the underwater streams.

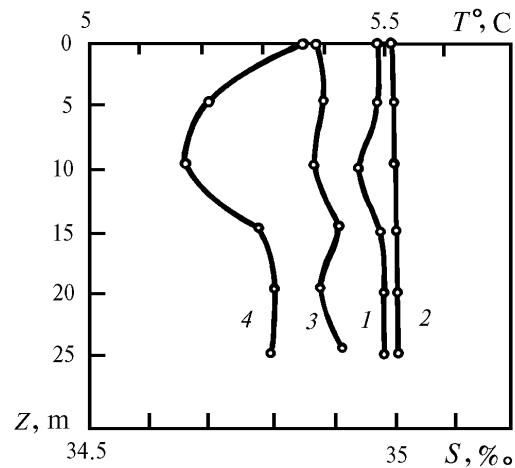


FIG. 1. Distribution of the temperature  $T$  (curves 1 and 3) and salinity  $S$  (curves 2 and 4) as functions of depth. Curves 1 and 2 are for station 2, curves 3 and 4 are for station 3.

As has already been noted, in the largest part of the region under study the water was homogeneous. The depolarization profiles typical of it are depicted in Fig. 2. Their qualitative pattern is in a good agreement with our previously obtained data.<sup>4</sup> True, the depolarization for the airborne lidar increases somewhat more rapidly which is natural. However, this difference is within the spread of the experimental data.

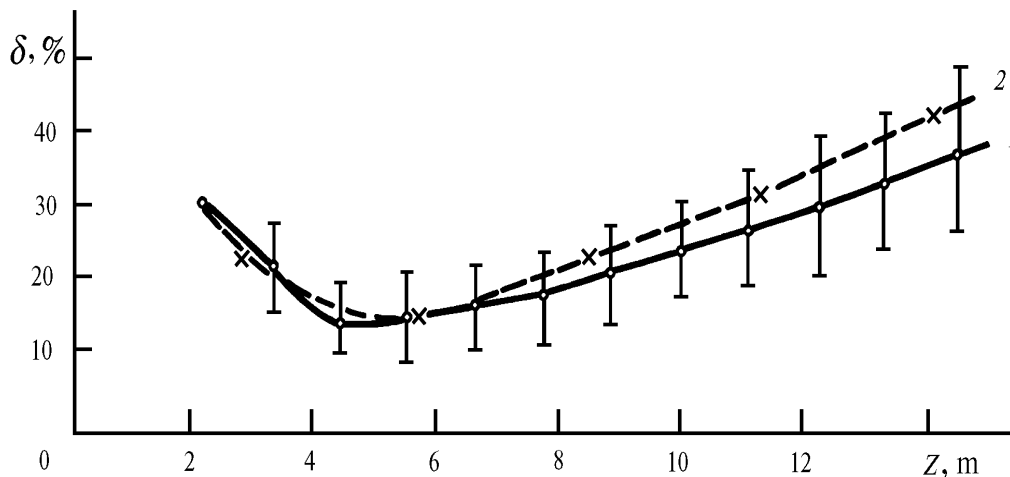


FIG. 2. Profiles of depolarization for homogeneous water as functions of depth. Curve 1 is for the shipboard lidar; curve 2 is for the airborne lidar.

In the region of local halocline at station 3 we observed spikes on the underwater portion of the airborne lidar returns at depths of 10–15 m. (The shipboard lidar was at a certain distance from the flight runs and did not record such pulses.) For about 70% of these signals the underwater pulses were detected only in the polarized component of lidar return; in 20% of all cases they were observed only in the depolarized component; and in 10% of all cases these peaks were recorded simultaneously in both components. The signal depolarization in this case was 35–40%. The percentage of pulses of different

shape remained unchanged when the flight altitude changed from 100 to 220 m.

As a whole, in the halocline the number of lidar returns with underwater pulses was 40% of the total number of signals for the airborne lidar.

The physical nature of such pulses with different states of polarization can be different and is outside the scope of this paper. (The PMT afterpulses were eliminated here.) Some prerequisites to such an analysis were undertaken by us elsewhere.<sup>14</sup>

The following conclusions can be drawn from this study, though, as has been noted above, the experiment cannot be thought of as being completed in full volume.

First, the sounding of homogeneous water using the aforementioned lidars gave both the radiation attenuation coefficients and the depolarization profiles close in values. This has given us the chance to complement them, use them simultaneously, retrieve data, and so on.

Second, an interesting effect has been observed in sounding of a local, on an ocean scale, inhomogeneity in the sea. This inhomogeneity about 30 km in size was manifested only by slightly increased salinity, without no evidence of the components whose phase composition differed from that of water. This halocline affected the optical parameters of water on even smaller scale since the shipboard lidar did not detect any optical anomalies while the airborne lidar did but in the mode of runs. Finally, some finer structure several tens and hundreds of meters in size was observed. Its cells altered differently the polarization state of lidar return from under the water.

All this inspires confidence that such experiments must be continued in spite of their complexity and high cost.

#### REFERENCES

1. D.V. Vlasov, *Izv. Akad. Nauk SSSR, Ser. Fiz.* **50**, No. 4, 724–735 (1986).
2. F.E. Hoge, C.W. Wright, W.B. Krabill, et al., *Appl. Opt.* **27**, No. 19, 3369–3977 (1988).
3. Yu.A. Gol'din and M.A. Evdoshenko, "Study of spatial variability of hydrooptical characteristics in frontal zones of the ocean," VINITI, No. 1654–B86, Moscow, February 24, 1986.
4. I.E. Penner, I.V. Samokhvalov, and V.S. Shamanaev, *Opt. Atm.* **1**, No. 12, 60–66 (1988).
5. S.A. Zenchenko, I.A. Malevich, V.I. Pranovich, et al., *Kvantovaya Elektron.* **14**, No. 11, 2381–2384 (1987).
6. A.I. Abramochkin, V.V. Zanin, I.E. Penner, et al., *Opt. Atm.* **1**, No. 2, 92–96 (1988).
7. V.E. Zuev, ed., *Laser Sounding of the Troposphere and Underlying Surface* (Nauka, Novosibirsk, 1987), 262 pp.
8. M.V. Kabanov, ed., *Remote Monitoring of the Upper Layer of the Ocean* (Nauka, Novosibirsk, 1991), 149 pp.
9. O.V. Kopelevich and V.K. Shemshura, *Okeanologiya* **23**, No. 5, 736–741 (1988).
10. M.V. Kozlyaninov, *Okeanologiya* **20**, No. 2, 329–334 (1980).
11. O. Steinvall, H. Klevebrant, J. Lexander, and A. Widen, *Appl. Opt.* **20**, No. 19, 3284–3286 (1981).
12. K.S. Shifrin, *Introduction into the Ocean Optics* (Gidrometeoizdat, Leningrad, 1983), 278 pp.
13. A. Gill, *Dynamics of the Atmosphere and Ocean* [Russian translation] (Mir, Moscow, 1986), Vol. 1, pp. 63–65.
14. M.M. Krekova, I.E. Penner, I.V. Samokhvalov, and V.S. Shamanaev, in: *Abstracts of Reports at the Ninth All-Union Symposium on Laser and Acoustic Sounding of the Atmosphere*, Tomsk (1987), Vol. 1, pp. 202–206.